Received: 9 April 2020 | Revised: 27 August 2020 | Accepted: 23 September 2020

DOI: 10.1111/ejn.14995

SPECIAL ISSUE ARTICLE

EJN European Journal of Neuroscience FENS WILEY

# Peripheral nerve regeneration following injury is altered in mice lacking P2X7 receptor

**Valerio Magnaghi**[1] | **Sarah Martin**[2] | **Patrick Smith**[2] | **Luke Allen**[2] | **Vincenzo Conte**[3] | **Adam J. Reid**[2,4] | **Alessandro Faroni**[2]

[1]Department of Pharmacological and Biomolecular Sciences, Università degli Studi di Milano, Milan, Italy

[2]Blond McIndoe Laboratories, Division of Cell Matrix Biology and Regenerative Medicine, School of Biological Sciences, Faculty of Biology Medicine and Health, University of Manchester, Manchester Academic Health Science Centre, Manchester, UK

[3]Department of Biomedical Sciences for Health, Università degli Studi di Milano, Milan, Italy

[4]Department of Plastic Surgery & Burns, Wythenshawe Hospital, Manchester University NHS Foundation Trust, Manchester Academic Health Science Centre, Manchester, UK

**Correspondence**
Alessandro Faroni, Blond McIndoe Laboratories, Division of Cell Matrix Biology and Regenerative Medicine, School of Biological Sciences, Faculty of Biology Medicine and Health, University of Manchester, Manchester Academic Health Science Centre, Manchester, UK.
Email: alessandro.faroni@manchester.ac.uk

**Funding information**
The Rosetrees Trust and the Stoneygate Trust, Grant/Award Number: M746; Academy of Medical Sciences, Grant/Award Number: AMS-SGCL7

**Editor:** Camilla Bellone

## Abstract

Peripheral nerve injuries are debilitating, and current clinical management is limited to surgical intervention, which often leads to poor functional outcomes. Development of pharmacological interventions aimed at enhancing regeneration may improve this. One potential pharmacological target is the P2X purinergic receptor 7 (P2X7R) expressed in Schwann cells, which is known to play a role during the development of the peripheral nerves. Herein, we analysed differences in regeneration between genetically engineered P2X7 knockout mice and wild-type controls, using in vivo and ex vivo models of peripheral nerve regeneration. We have found that the speed of axonal regeneration is unaltered in P2X7 knockout mice, nevertheless regenerated P2X7 knockout nerves are morphologically different to wild-type nerves following transection and immediate repair. Indeed, the detailed morphometric analysis at 4 and 8 weeks after injury showed evidence of delayed remyelination in P2X7 knockout mice, compared to the wild-type controls. Furthermore, the Wallerian degeneration phase was unaltered between the two experimental groups. We also analysed gene expression changes in the dorsal root ganglia neurones as a result of the peripheral nerve injury, and found changes in pathways related to pain, inflammation and cell death. We conclude that P2X7 receptors in Schwann cells may be a putative pharmacological target to control cell fate following injury, thus enhancing nerve re-myelination.

**KEYWORDS**

axon, cytokine, myelin, Schwann cell, unmyelinated fibres

**Abbreviations:** Ach, Acetylcholine; ATF3, activating transcription factor 3; ATP, adenosine triphosphate; BDNF, brain derived neurotrophic factor; CASP2, caspase-2; CASP3, capsase-3; DRG, dorsal root ganglion; GABA, γ-aminobutyric acid; GAL, galanin; GAP43, growth associated protein 43; IC, circularity index; MAG, myelin associated glycoprotein; MBP, myelin basic protein; NGF, nerve growth factor; P0, myelin protein zero; P2X7R, P2X purinergic receptor 7; PBS, phosphate buffered saline; TBST, tris-buffered saline-Tween; WD, Walerian degeneration; WT, wild type.

# 1 | INTRODUCTION

Peripheral nerve injuries, occurring as a result of trauma to upper and lower limbs, are common and debilitating. The most severely affected patients may face permanent disability, chronic pain, and psychological challenges. Current treatments, merely limited to surgical repair, are ineffective and lead to poor functional recovery (Zochodne, 2012). There are no pharmacological interventions that can improve regeneration and repair; however, several molecules and receptors, targeting mainly Schwann cells, have been suggested as potential candidates for pharmaceutical therapies (Magnaghi et al., 2009). These pharmacological strategies to enhance nerve regeneration include the use of neurosteroids, neurotransmitters and other small molecules (Martinez de Albornoz et al., 2011). Indeed, research has shown that receptors for neurotransmitters such as γ-aminobutyric acid (GABA), Acetylcholine (Ach), and adenosine triphosphate (ATP), are able to modulate physiological parameters in Schwann cells, which may be exploited to improve peripheral nerve regeneration outcomes (Faroni, Castelnovo, et al., 2014; Faroni, Smith, et al., 2014; Uggenti et al., 2014). Mice lacking receptors for GABA, Ach and ATP have shown an altered peripheral nerve development, that results in specific peripheral nervous system (PNS) phenotypes (Faroni, Smith, et al., 2014; Magnaghi et al., 2008; Uggenti et al., 2014).

The P2X purinergic receptor 7 (P2X7R) is a plasma membrane ligand-gated ion channel operated by ATP. In Schwann cells, these receptors bind ATP released from dorsal root ganglia (DRG) and axons in an activity-dependent manner; however, the effects of ATP on downstream purinergic signalling pathways involved in peripheral nerve regeneration, myelination and function are largely unknown (Fields & Stevens, 2000; Stevens & Fields, 2000; Stevens et al., 1998). Previous work by our group has shown that P2X7R is expressed predominantly in myelinating Schwann cells and that, during development, lack of P2X7R causes Schwann cells to commit to a non-myelinating phenotype (Faroni, Smith, et al., 2014). These results were obtained by studying P2X7R knockout mice developed by GlaxoSmithKline (GSK) (Chessell et al., 2005); however, another mouse strain with ablation of P2X7R was developed by Pfizer Inc. (Solle et al., 2001), and the two models have been reported to possess similar, although not identical, phenotypes (Sim et al., 2004). In the current study, we aimed to confirm the PNS phenotype, we previously observed in the GSK mouse model, in Pfizer's mice strain. Moreover, we aimed to determine whether P2X7R affects the speed of degeneration, regeneration and myelin formation following nerve transection. This will be done through characterising the differences between genetically engineered P2X7R knock out (KO) mouse model, and wild-type (WT) controls, in ex vivo and in vivo models of peripheral nerve injury and repair.

# 2 | MATERIALS AND METHODS

## 2.1 | Experimental mice and surgical procedures

All animal experiments were performed in accordance with the UK Animals (Scientific Procedures) Act, 1986. Pfizer P2X7 KO mice (B6.129P2-P2rx7$^{tm1Gab}$/J) were acquired from The Jackson Laboratory, US (Solle et al., 2001). C57BL/6 mice obtained from the Biological Service Facility of the University of Manchester were used as WT controls. All mice were 3–4 month old males. For surgical transection, animals were anaesthetised with isoflurane and the sciatic nerves were transected. Immediately following transection the sciatic nerves were repaired with 11-0 sutures under an operating microscope (Leica, UK). For the non-repair group, the proximal and distal stumps of sciatic nerve were sutured to an adjacent muscle. One week after the axotomy and no repair surgery, mice underwent terminal anaesthesia with carbon, dioxide ($CO_2$) and cervical dislocation. The lumbar 4 and 5 DRGs were removed via cutting of the central and peripheral branch, close to the ganglia. The DRGs were harvested from the injured (lnj) and the contralateral control side (Ctrl) in all mice (P2X7 KO and WT). Samples were collected with $n = 5$ for the four groups and stored at −40°C until real time PCR analyses. For the injury and repair experiments, tissues were collected at 1 and 2 weeks and processed for immunohistochemistry ($n = 5$). Furthermore, we performed long term studies at 4 and 8 weeks survival for morphometric analyses through transmission electron microscopy analyses ($n = 4$).

## 2.2 | Genotyping

Ear clippings from KO and WT animals were lysed for 2 hr at 55°C and DNA was isolated by adding phenol:chloroform:isoamyl alcohol solution (25:24:1; Sigma-Aldrich, UK). Lysis buffer was: 100 mM NaCl, 10 mM Tris Buffer, 1 mM EDTA, 1% SDS, 0.1 mg/ml Proteinase K (all from Sigma-Aldrich). For polymerase chain reaction (PCR), each well contained 1 μl of extracted DNA and 9 μl master mix (5X Green GoTaq Flexi buffer, $MgCl_2$ 2 mM, dNTPs 0.2 mM, primers mix 0.5 μM each, GoTaq DNA polymerase 5 U/μl; Promega, Southampton, UK). Primers were obtained from Sigma and sequences were as follows: WT allele: 5′–TGG ACT TCT CCG ACC TGT CT–3′ and 5′–TGG CAT AGC ACC TGT AAG CA–3′; KO allele: 5′–CTT GGG TGG AGA GGC TAT TC–3′ and 5′–AGG TGA GAT GAC AGG AGA TC–3′. The PCR protocol

used can be found on the Jackson Laboratories website, and it involved 28 cycles of 94°C for 15 s, annealing at 50°C for 15 s, and extension at 72°C for 10 s; followed by 72°C of final extension for 2 min and hold at 4°C. Following PCR, samples were loaded onto a 1.5% agarose gel and were run at 80V for 1.5 hr before analysis with an AlphaImager 2200 gel documentation system (Alpha Innotech/Proteinsimple, Santa Clara, CA, USA).

## 2.3 | Western blot

Sciatic nerves were first homogenised using a tissue ruptor (Qiagen, Manchester, UK) and left to lyse on ice in lysis buffer for 30 min. Samples were then freeze/thawed and centrifuged at 13,000 *g*, 4°C, for 15 min (IEC CL31R Multispeed; Fisher Scientific, Loughborough, UK) before separating the supernatant from the pellet. Supernatant protein concentration was determined using the Bio-Rad detergent-compatible protein assay (Bio-Rad Laboratories, Hemel Hempstead, UK) and standard curve of bovine serum albumin (BSA; Sigma-Aldrich) standards, and a spectrophotometer (Asys UVM340 Microplate Reader; Bichrom, Cambridge, UK). Ten micrograms of protein from each sample were mixed with loading buffer (2X buffer: Tris-HCl 100 mM, pH 6.8, SDS 4% (w/v), bromophenol blue 0.2% (w/v), glycerol 20% (v/v), β-mercaptoethanol 200 mM; Sigma-Aldrich), and boiled at 100°C for 3 min, followed by centrifugation at 13,000 *g* at room temperature for 1 min. Samples were loaded onto a 10% polyacrylamide gel (40% acrylamide 29:1; Sigma-Aldrich) with protein marker (ColorPlus prestained protein marker, 8–175 kDa; New England Biolabs, Hitchen, UK) and ran for 90–120 min at 80–120 V. Gels were transferred onto a nitrocellulose membrane (Amersham Hybond-ECL; GE Healthcare, Little Chalfont, UK) with a Bio-Rad wet transfer apparatus (transfer buffer: Tris-base 25 mM, glycine 192 mM, methanol 20% (v/v) at 80 V for 1 hr. To confirm protein transfer membranes were then treated with ponceau red (ponceau 0.1% (w/v), acetic acid 0.5% (v/v)). Membranes were blocked in 5% (w/v) skimmed milk in tris-buffered saline-Tween (TBST; Tween-20 0.5% (v/w), NaCl 140 mM, Tris 10 mM, pH 7.5) for 30–60 min and incubated in primary antibodies overnight at 4°C on a shaker. The following day membranes were washed for 30 min in TBST, incubated in horseradish peroxidase (HRP)-conjugated secondary antibodies at room temperature for 1 hr, and washed for 30 min in TBST. Primary antibodies were used at the following dilutions: anti-protein zero (P0), 1:200 (Abcam, UK); anti-myelin basic protein (MBP), 1:200 (Millipore, UK); anti-myelin associated glycoprotein (MAG), 1:200 (Cell Signalling Technologies, UK). Rabbit secondary -HRP antibodies were used 1:500 (Cell Signalling Technologies, UK). Membranes were treated with pico- or femtochemiluminescence mixes (SuperSignal West pico/femto chemiluminescent substrate; Fisher Scientific) for 5 min for signal detection. Luminescent bands were imaged using a Kodak Image Station 4000mm PRO. Densitometry analysis was performed in Image J (version 1.47f, NIH, USA). Bands were normalised to the housekeeping protein β-tubulin data was expressed as the percentage versus the WT control.

## 2.4 | Immunohistochemistry

Following overnight fixation in 4% (w/v) paraformaldehyde (PFA) at 4°C, sciatic nerves were cryoprotected in 15% (w/v) sucrose in phosphate buffered saline (PBS) which was replaced daily for 3 days. Nerves were embedded in optimal cutting temperature embedding matrix (Raymond A Lamb, Eastbourne, UK), and stored at −80°C until further processing. Nerves were then sliced into 15 μm longitudinal sections using a cryostat (OTF; Bright Instruments, Cambridgeshire, UK) set at −20°C. Slices were dried overnight at 37°C, before permeabilisation in 0.2% (v/v) Triton X-100 in PBS for 1 hr at room temperature, and a further two washes in PBS for 5 min. Sections were then blocked in 5% blocking serum (Normal Goat Serum, Sigma) diluted 1:100 in antibody diluent (0.03% (v/v) Triton, 0.10% (w/v) BSA, 0.10% (**w/v**) sodium azide) for 1 hr at room temperature. Sections were then incubated in a rabbit primary antibody labelling neurofilament 200 (NF200, Sigma-Aldrich) overnight at 4°C. After incubation, sections were washed in PBS for 5 min twice, incubated in Alexa-488 labelled anti-rabbit secondary antibody raised in goat (Thermo Scientific, UK) for 2 hr at room temperature and in dark conditions, and then washed twice in PBS for 5 min. Finally, coverslips were fitted to the slides using Vectashield with 4′,6-diamidino-2-phenylindole (DAPI) H-1200 (Vector Laboratories, Peterborough, UK). Fluorescence microscopy analysis was performed with an Olympus BX60 fluroscence microscope, and images were recorded in Image ProPlus v 6.0 (Media Cybernetics, Rockville, MD, USA). Tiled images were merged using Photoshop CS6 (Adobe).

## 2.5 | Explant culture as Wallerian Degeneration (WD) Model

Following terminal anesthesia using carbon dioxide ($CO_2$) and cervical dislocation, approximately a 10 mm segment of the sciatic nerves (from both legs) were removed from both P2X7 KO and WT mice ($n = 3$). Three nerve segments from each group nerve were frozen immediately in liquid nitrogen to ensure Wallerian degeneration could not occur. These samples are referred to as time zero (T0). Contralateral KO and WT sciatic nerves were divided into 1–2 mm long

sections and cultured as floating nerve explants in Dulbecco's modified eagles medium (Sigma), containing 10% (v/v) fetal bovine serum (Labtech), 2% (v/v) L-glutamine (sigma) and 1% (v/v) penicillin-streptomycin (Sigma). The cultures were maintained at 37°C in a humidified atmosphere containing 5% Carbon dioxide ($CO_2$) for 72 hr to recapitulate Wallerian degeneration ex vivo. After culture, samples were then frozen using liquid nitrogen and stored in a −40°C freezer until real time PCR analyses. These samples are referred to as T72 (time point 72 hr).

## 2.6 | Real-time quantitative polymerase chain reaction

The RNeasy lipid tissue mini kit (Qiagen) was used for the extraction of RNA from the sciatic nerves and DRG samples. Tissues were homogenised using the Qiagen Tissue Ruptor (for nerves) or mortar and pestle (DRG). Chloroform was then added and the tissue was centrifuged at 120,000 *g* for 15 min to separate the nucleic acids in the aqueous phase. Following ethanol addition, the mixture was applied to RNeasy spin column to purify RNA and get rid of contaminants. The concentration of RNA obtained from both tissues types was then determined by the measuring the absorbance at 260 nm using a Nanodrop-1000 spectrophotometer (Thermo Scientific). The extracted RNA was reverse transcribed using the $RT^2$ First Strand Kit (Qiagen) and a PTC-200 Peltier Thermal Cycler (MJ Research) according to the manufacturer's instructions. Either 100 ng (DRG) or 140 ng (nerves) of RNA were reverse transcribed. Primers for RT-PCR are listed in Table 1. PCR reactions were performed with a Corbett Research thermocycler, using ad $RT^2$ SYBR Green kit (Qiagen), and data were

**TABLE 1** Table of primers used in real time-PCR studies

| Gene | Primer sequence (5′–3′) | PL (bp) | Reference |
|---|---|---|---|
| CASP2 | FW: CCACAGATGCTACGGAACA<br>RV: GCTGGTAGTGTGCCTGGTAA | 99 | Hanoux et al. (2007) |
| CASP3 | FW: TGCAGCATGCTGAAGCTGTA<br>RV: GAGCATGGACACAATACACG | 150 | Gesing et al. (2015) |
| ATF3 | FW: GCTGCCAAGTGTCGAAACAAG<br>RV: CAGTTTTCCAATGGCTTCAGG | 331 | Allen-Jennings et al. (2001) |
| GAP43 | FW: TGTGGGAGTCCACTTTCCTC<br>RV: GAACGGAACATTGCACACAC | 64 | Namsolleck et al. (2013) |
| NGF-B | FW: CCAGTGAAATTAGGCTCCCTG<br>RV: CCCTTGGCAAAACCTTTATTGGG | 143 | Namsolleck et al. (2013) |
| GAL | FW: TGGAGGAAAGGAGACCAGGAAG<br>RV: GCCTCTTTAAGGTGCAAGAAACTG | 100 | He et al. (2005) |
| NFkB | FW: CTACGGAACTGGGCAAATGT<br>RV: TCGAAATCCCCTCTGTTTTG | 145 | Nagajyothi et al. (2012) |
| TNFa | FW: CCGATGGGTTGTACCTTGTC<br>RV: GTGGGTGAGGAGCACGTAGT | 77 | Cunningham et al. (2002) |
| 18S | FW: CTGCCCTATCAACTTTCGATGGTAG<br>RV: CCGTTTCTCAGGCTCCCTCTC | 100 | Faroni, Smith, et al. (2014) |
| MAG | FW: CACCTTCTCGGAGCACAG<br>RV: GTTCCTGCCACCACTTCC | 78 | Faroni, Smith, et al. (2014) |
| MBP | FW: AGGACTCACACACGAGAACTACCC<br>RV: GGTGTTCGAGGTGTCACAATGTTC | 121 | Faroni, Smith, et al. (2014) |
| PMP22 | FW: CGGTTTTACATCACTGGATTCTTC<br>RV: TTGACATGCCACTCACTGT | 98 | Faroni, Smith, et al. (2014) |
| P0 | FW: TGACAACGGCACTTTCACA<br>RV: TCCCAACACCACCCCATA | 118 | Faroni, Smith, et al. (2014) |
| BDNF | FW: GGTATCCAAAGGCCAACTGA<br>RV: CTTATGAATCGCCAGCCAAT | 183 | Faroni, Smith, et al. (2014) |

analysed with RotorGene-6000 series software (version 1.7). The PCR conditions were set to: 1 step at 95°C for 10 min to activate the HotStart DNA Taq Polymerase, followed by 40 cycles of 15 s at 95°C, 30 s at 55°C and 30 s at 72°C, where the fluorescence data were collected. The protocol was terminated with a melting curve program of 95°C for 1 min, 65°C for 2 min, and gradual change from 65°C to 95°C, with a 1°C increase at each step. Data were analysed via the ΔΔCt method, and normalised for the housekeeping gene (18s) and the control groups (uninjured control and T0 control nerves).

## 2.7 | Transmission electron microscopy

Following terminal anaesthesia and cervical spine dislocation, mice were perfused transcardially with 2% paraformaldehyde and 2% glutaraldehyde in sodium cacodilate buffer (0.1 M, pH 7.3) for fixation. The sciatic nerves were then harvested and immersed in the same fixative solution overnight at 4°C. Samples were postfixed in 2% $OsO_4$ (Sigma-Aldrich), washed in distilled water, stained with 2% aqueous uranyl acetate, dehydrated in graded alcohol and embedded in Epon-Araldite resin. Ultrathin sections (ca. 70–80 nm) of the fixed sciatic nerves were collected on formvar coated single slot grids and counterstained with lead citrate, then examined with a Zeiss EM 10 electron microscope (Oberkochen, Germany). For morphological analysis, more than 25% of the total cross-sectional area of each nerve (corresponding to at least 25% of the total nerve cross-sectional area, about 90–100 fields) were randomly selected using a systematic random-square sampling method throughout the entire nerve profile (Mayhew & Sharma, 1984) and Image Pro-Plus 6.0. The measurement of myelinated fibres (at least 1,500 fibres/animal), myelin thickness, G-ratio (ratio between inner axonal diameter and total outer diameter of the fibre) and irregular fibres [index of circularity (IC), calculated as squared fibre perimeter/4π fibre area, <0.75] were assessed. The number of Remak bundles, number of unmyelinated axons in each bundle, number of single unmyelinated and myelinated axons were counted. Data were expressed per unit of surface area (100 $\mu m^2$) ± *SEM*.

## 2.8 | Statistical analysis

All statistical analyses were performed using GraphPad Prism (version 8.2.1 for Mac; GraphPad Software, San Diego, CA, USA). Statistical significance was evaluated by two-tailed unpaired *t* tests or two-way ANOVA. Results were considered significant at $p < 0.05$.

# 3 | RESULTS

## 3.1 | Confirming PNS phenotype in Pfizer's $P2X_7R$ knockout mouse strain

Pfizer's P2X7 knockout (KO) mice (3-month-old males) were sourced from The Jackson Laboratory (B6.129P2-P2rx7$^{tm1Gab}$/J), and C57BL/6 wild type (WT) were used as controls. Firstly, we demonstrated the ablation of P2X7R by using specific primer sequences. Indeed, PCR analyses performed on tail biopsies or ear punches confirmed that the experimental mice express the KO sequence (280 bp), and not the WT sequence (363 bp). All control mice express the WT P2X7 sequence (363 bp), and heterozygote mice express both the WT and KO sequence (280 and 363 bp, Figure 1a).

Since significant differences have been reported in GSK and Pfizer's P2X7 KO mice (Sim et al., 2004), we proceeded to confirm the PNS phenotype we previously reported in GSK mice (Faroni, Smith, et al., 2014), in the newly acquired Pfizer model. Interestingly, we observed significant reduction of the protein levels of the main peripheral myelin proteins P0 (****$p < 0.0001$), MBP (*$p < 0.05$) and MAG (**$p < 0.01$) using western blot analyses (Figure 1b). Moreover transmission electron microscopy analyses confirmed the altered morphology of P2X7 KO mice, which feature a significantly higher number of Remak bundles (***$p < 0.001$), containing a higher number of unmyelinated axons (***$p < 0.001$, Figure 1c). Albeit not statistically significant, P2X7R knockout mice showed a reduced myelinated/unmyelinated axon ratio compared to WT controls, but the overall myelin thickness was unaltered. Finally, the percentage of irregular fibres, with circularity index (IC) lower than 0.75, was significantly higher in P2X7R knockout mice compared to WT controls (*$p < 0.05$).

## 3.2 | Gene expression changes in DRG neurons following nerve transection

Given that peripheral nerve injury is accompanied with profound changes in gene expression at the level of the DRG neurons (Martin et al., 2019), we investigated if some of these changes could be affected by the absence of P2X7R. We analysed the expression levels for markers of cell death, inflammation, survival and regeneration in DRG by real-time PCR, 1 week after peripheral nerve transection and no repair (Figure 2a). Peripheral nerve injury caused an increase in caspase 2 (CASP2) gene expression level in DRG from both WT (ns) and P2X7 KO (**$p < 0.01$) mice, as well as an increase in caspase 3 (CASP3, ****$p < 0.0001$ WT; ***$p < 0.001$ P2X7 KO) gene expression levels (Figure 2b).

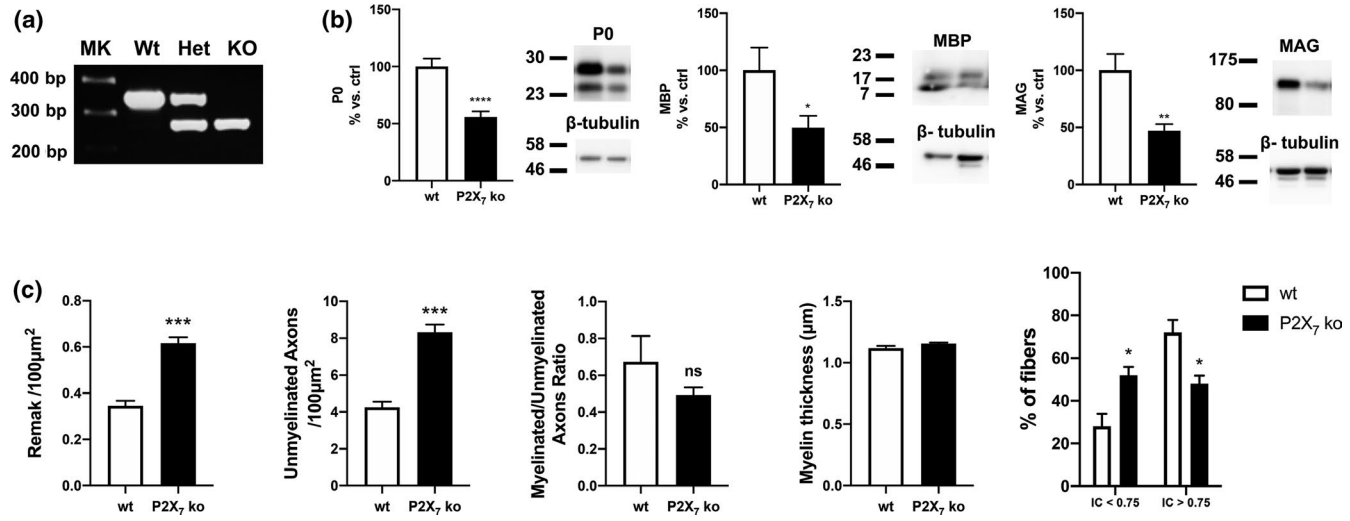


**FIGURE 1** P2X7R knockout mice display different morphological characteristics compared to wild type controls. (a) Confirmation of ablation of the complete P2X7R sequence was performed by PCR using specific primers; KO mice only showed KO sequence of 280 bp, whereas in control mice only the WT amplicon (363 bp) was generated. Heterozygous mice showed both amplicons. (b) Western blot analysis of sciatic nerve homogenates taken from P2X7 KO mice showed that these animals express significantly less P0 (56 ± 4.96% versus WT, $^{****}p < 0.0001$), MBP (49.8 ± 10.2% versus WT, $^{*}p < 0.05$), and MAG (47.2 ± 5.63% versus WT, $^{**}p < 0.01$), when compared to the control WT animals. (c) Transmission electron microscopy (TEM) analysis of sciatic nerves revealed significant morphological differences between KO and control WT nerves. P2X7 KO nerves showed a higher number of Remak bundles compared to WT mice (0.617 ± 0.026 versus 0.345 0.022 per 100 µm$^2$, $^{***}p < 0.001$). The Remak bundles also contained a significantly higher number of unmyelinated axons (8.314 ± 0.428 versus 4.424 ± 0.309 per 100 µm$^2$, $^{***}p < 0.001$). The ratio between myelinated and unmyelinated axons was lower in KO compared to WT controls, although this was not statistically significant (0.493 ± 0.041 KO versus 0.673 ± 0.140 WT, ns). We found no significant differences in myelin thickness (1.118 ± 0.019 µm WT versus 1.156 ± 0.008 µm KO, ns). The percentage of irregular fibres with circularity index (IC) lower than 0.75 was significantly higher in the KO nerves compared to WT (52 ± 3.907% versus 28 ± 5.925%, $^{*}p < 0.05$)

Markers of inflammation were also upregulated in DRG after nerve transection in both WT and P2X7R KO mice (Figure 2c). Indeed, nuclear factor kappa-light-chain-enhancer of activated B cells (NFkB) levels were marginally increased after injury in WT mice (ns), whereas in P2X7 KO the increase was statistically significant ($^{**}p < 0.01$). Conversely, tumour necrosis alpha (TNFα) expression levels were significantly increased after injury in WT mice ($^{*}p < 0.05$), but only marginally increased in P2X7 KO (ns).

Furthermore, we analysed markers of survival, nerve function and nociception such as Activating Transcription Factor 3 (ATF3), Growth Associated Protein 43 (GAP43), Nerve Growth Factor (NGF) and galanin (GAL, Figure 2d). Nerve transection caused a significant increase in the expression

**FIGURE 2** Gene expression changes in DRG following peripheral nerve transection and no repair. (a) Sciatic nerves from WT and P2X7 KO mice were transected with no attempted repair and DRG were harvested 1 week following the injury to analyse gene expression changes ($n = 5$). (b) CASP2 was upregulated in DRG after the peripheral injury compared to DRG from uninjured mice (WT: 1.270 ± 0.137 fold change versus 1.000 ± 0.13, ns; KO: 1.460 ± 0.082 fold change versus 0.836 ± 0.057, $^{**}p < 0.01$). CASP3 was also upregulated in DRG after injury (WT: 3.928 ± 0.357 fold change versus 1.000 ± 0.142, $^{****}p < 0.0001$; KO: 3.360 ± 0.552 fold change versus 0.548 ± 0.045, $^{***}p < 0.001$). (c) The increase in NFkB expression after injury was only marginal in DRG from WT mice (1.440 ± 0.162 fold change versus 1.000 ± 0.098, ns), whereas it was statistically significant in P2X7 KO mice (1.686 ± 0.161 fold change versus 0.888 ± 0.053, $^{**}p < 0.01$). TNFα expression was increased in DRG from injured groups in both WT (4.652 ± 1.501 fold change versus 1.367 ± 0.396, $^{*}p < 0.05$) and P2X7 KO mice strain (2.854 ± 0.589 fold change versus 0.987 ± 0.210, ns). (d) ATF3 was significantly upregulated in injured DRGs from both groups (WT: 107.540 ± 15.412 fold change versus 1.000 ± 0.176, $^{****}p < 0.0001$; KO: 72.886 ± 10.243 fold change versus 0.616 ± 0.143, $^{***}p < 0.001$). GAP43 also followed a similar trend (WT: 4.916 ± 0.785 fold change versus 1.000 ± 0.224, $^{**}p < 0.01$; KO: 5.836 ± 0.937 fold change versus 0.984 ± 0.107, $^{***}p < 0.001$). Similarly, NGF expression was upregulated in both WT (3.152 ± 0.535 fold change versus 1.000 ± 0.286, $^{**}p < 0.01$) and P2X7 KO (1.984 ± 0.361 fold change versus 0.532 ± 0.090, $^{*}p < 0.05$) DRGs from the injured groups. Finally, DRGs from injured WT mice expressed significantly more GAL compared to uninjured controls (28.000 ± 4.288 fold change versus 1.000 ± 0.091, $^{****}p < 0.0001$), similarly to P2X7 KO mice (47.570 ± 3.515 fold change versus 1.004 ± 0.116, $^{****}p < 0.0001$). Interestingly, GAL expression levels were significantly higher in injured P2X7 KO compared to injured WT DRGs ($^{***}p < 0.001$)

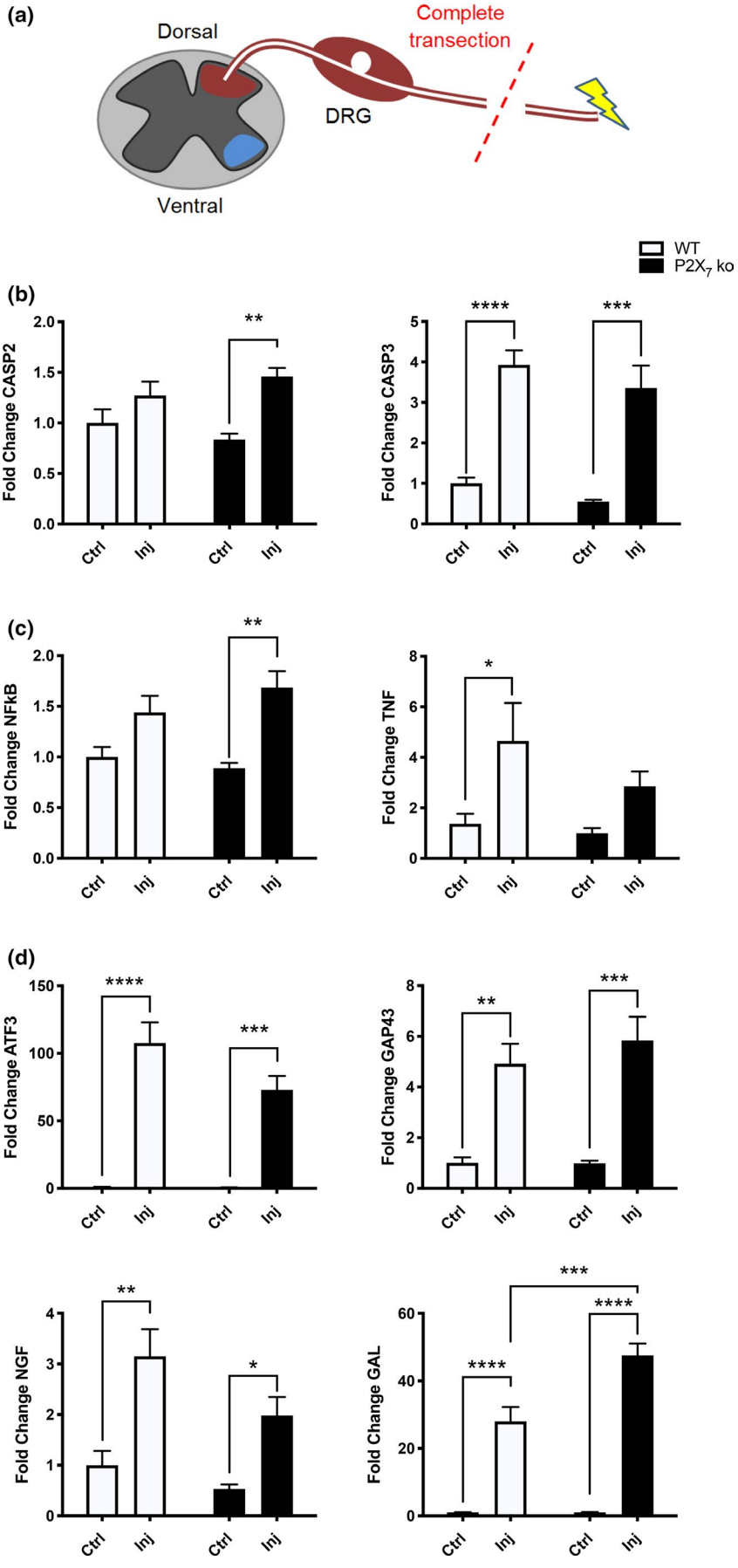
(a)
Dorsal
Complete transection
DRG
Ventral
WT
P2X7 ko
(b)
Fold Change CASP2
Fold Change CASP3
(c)
Fold Change NFkB
Fold Change TNF
(d)
Fold Change ATF3
Fold Change GAP43
Fold Change NGF
Fold Change GAL
Ctrl
Inj

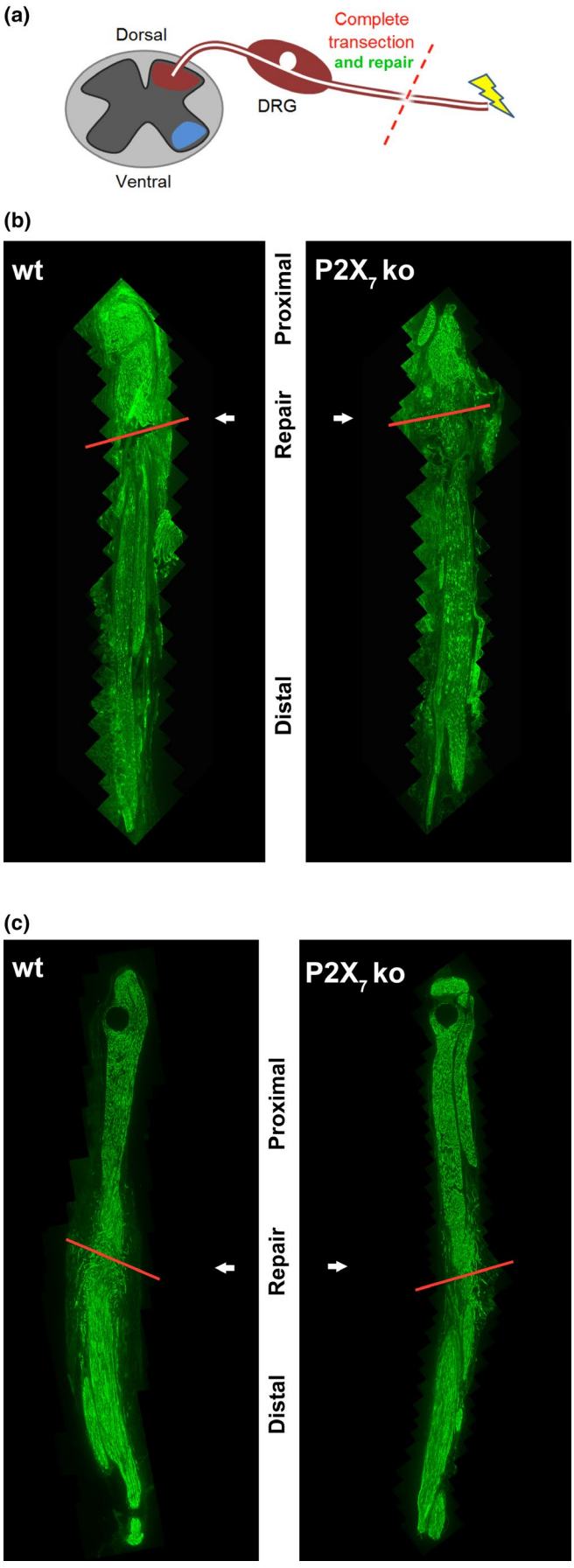


**FIGURE 3** Speed of degeneration and regeneration is unaltered in P2X7 KO mice. (a) Sciatic nerves were cut and immediately repaired in both experimental groups ($n = 5$) and regeneration was assessed after 1 and 2 weeks. (b) Immunohistostaining of NF200 (green) following 1 week survival highlighted axonal growth at the injury site (red line) and degenerating axons in the distal stump. We observed no differences in the histological features of the degenerating nerves between the experimental (right) and the control (left) groups. (c) Similarly, 2 weeks after the repair the axons had regenerated throughout the distal stump, and no differences in regeneration speed was observed between the control (WT, left) and experimental groups (P2X7 KO, right)

levels of ATF3 in the DRGs of both WT (****$p < 0.0001$) and P2X7 KO mice (***$p < 0.001$). Similarly, levels of GAP43 were significantly increased in WT (**$p < 0.01$) and P2X7 KO (***$p < 0.001$) DRGs after injury. NGF was also upregulated in DRG after injury in both WT (**$p < 0.01$) and KO (*$p < 0.05$) groups. Overall, no major differences in the expression levels were observed between the WT and KO mice. Nevertheless, we found increased expression levels of the neuropeptide GAL in both WT (****$p < 0.0001$) and P2X7 KO DRGs (****$p < 0.0001$) after injury, and GAL expression levels were significantly higher in injured P2X7 KO DRGs compared to injured WT (***$p < 0.001$).

### 3.3 | Degeneration and regeneration speed are not affected by P2X7R absence

To assess the effect of P2X7R ablation on the efficacy of nerve regrowth we performed a sciatic nerve transection with immediate repair, and performed histological analyses on longitudinal nerve sections 1 and 2 weeks after survival (Figure 3a). One week after the injury and repair, evidence of growing axonal cones could be observed (neurofilament 200 staining, NF200, green) at the injury/repair site (red line); whereas in the distal stump the distribution of the axonal debris suggested ongoing Wallerian degeneration, without major differences between the WT and P2X7 KO groups (Figure 3b). Following 2 weeks survival, NF200 staining (green) showed complete regeneration of newly formed axons within the distal stump in both experimental groups (Figure 3c).

To confirm that WD is not affected by the absence of P2X7R, we performed gene expression analyses in an ex vivo model of WD. We chose an ex vivo, rather than in vivo model in order to minimise the systemic effects of P2X7R ablation, and focus on the effects of P2X7R removal mainly in Schwann cells. Sciatic nerves were collected from WT and P2X7 KO mice, and cultured as explants for 72 hr to recapitulate WD in vitro.

We started by analysing the levels of the main myelin proteins in the peripheral nerves: MAG, MBP, PMP22 and P0. Freshly isolated sciatic nerves (T0) from P2X7 KO mice expressed significantly higher levels of MAG (**$p < 0.01$, Figure 4a). Following 72 hr of in vitro WD (T72), MAG expression levels were significantly decreased in both WT and P2X7 KO nerves (****$p < 0.0001$, Figure 4a). Basal MBP gene expression levels were similar in WT and P2X7 KO (ns, Figure 4b), and following 72 hr of degeneration in vitro MBP expression was significantly decreased in both

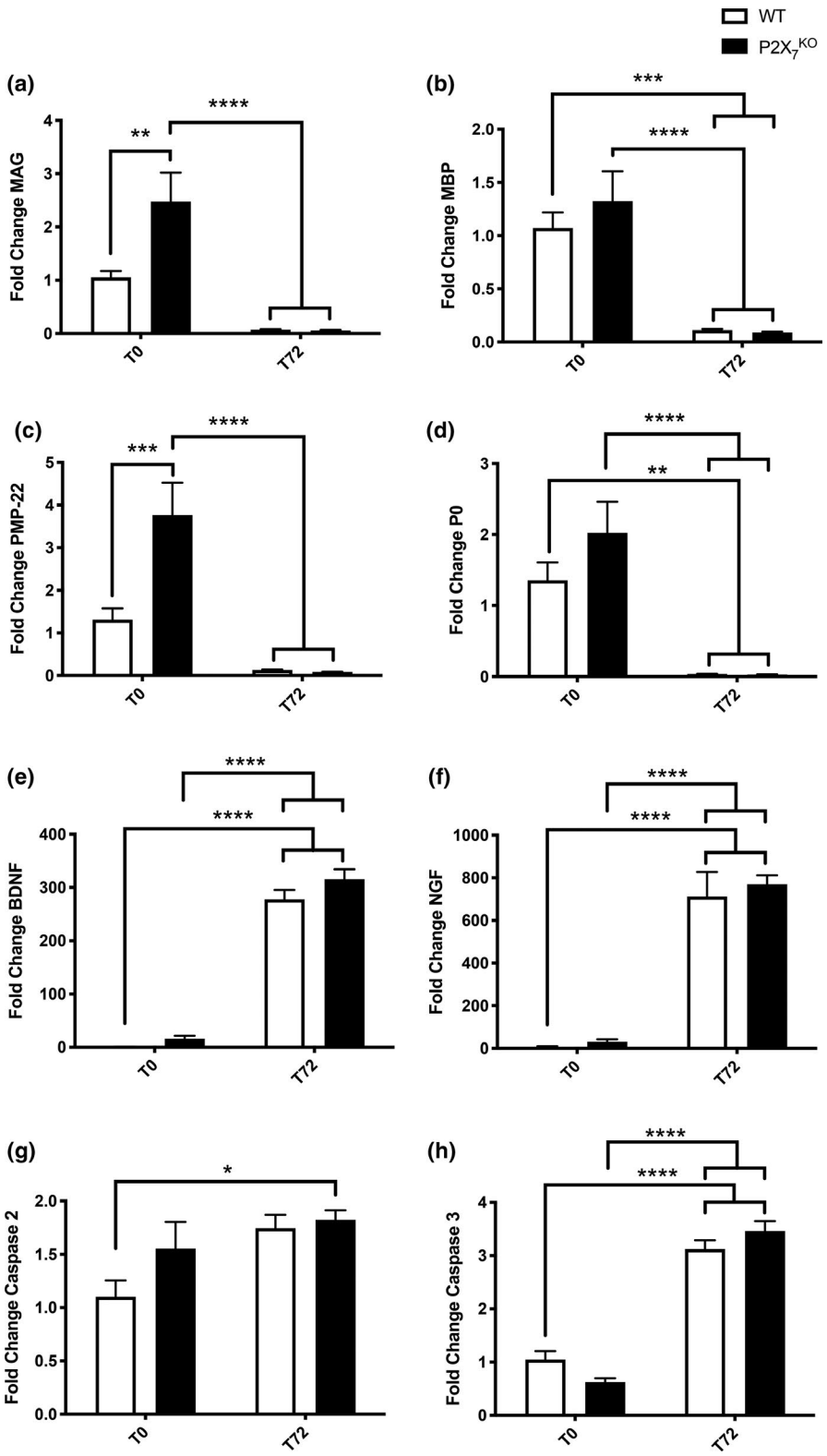

**FIGURE 4** Wallerian degeneration is similar in WT and P2X7 KO mice. (a) Gene expression analyses showed that basal MAG levels (T0) were higher in P2X7 KO nerves compared to controls (2.474 ± 0.546 fold increase versus 1.051 ± 0.119, $^{**}p < 0.01$). Nerves were left to degenerate for 72 hr (T72) in vitro to recapitulate Wallerian degeneration (WD) and MAG expression levels were significantly decreased in both experimental groups (0.068 ± 0.010 and 0.059 ± 0.006 for WT and P2X7R KO respectively, $^{****}p < 0.0001$). (b) MBP levels were similar at T0 between WT and KO groups (1.073 ± 0.147 versus 1.324 ± 0.280, ns), and significantly decreased following 72 hr: 0.112 ± 0.010 in WT ($^{***}p < 0.001$); and 0.092 ± 0.007 in P2X7 KO nerves ($^{****}p < 0.0001$). (c) PMP22 levels were significantly higher in P2X7 KO at T0 versus WT (3.765 ± 0.758 fold change versus 1.311 ± 0.265, $^{***}p < 0.001$), and greatly decreased after 72 hr of degeneration in vitro (0.121 ± 0.014 WT, and 0.085 ± 0.005 P2X7 KO, $^{****}p < 0.0001$). (d) P2X7R KO nerves expressed slightly higher levels of P0 compared to WT (2.025 ± 0.438 fold change versus 1.355 ± 0.253, ns), and after 72 hr P0 levels were significantly decreased in both WT (0.035 ± 0.003, $^{**}p < 0.01$) and P2X7 KO (0.030 ± 0.002, $^{****}p < 0.0001$). (e) P2X7 KO nerves showed higher levels of BDNF (15.745 ± 5.770) compared to WT nerves (1.114 ± 0.191), although this was not statistically significant (ns). Following degeneration, BDNF levels significantly increased in both WT (277.367 ± 18.096) and P2X7 KO nerves (315.461 ± 18.815, $^{****}p < 0.0001$). (f) NGF expression was higher in KO nerves compared to WT (30.757 ± 11.008 fold change versus 6.585 ± 3.539, ns), and it significantly increased in both WT (712 ± 115.285, $^{****}p < 0.0001$) and P2X7 KO (769 ± 42.678, $^{****}p < 0.0001$) nerves. (g) WT and KO nerves expressed similar levels of CASP2 (1.101 ± 0.153 versus 1.553 ± 0.251, respectively); expression levels did not significantly change following ex vivo WD (1.744 ± 0.153 and 1.824 ± 0.089 for WT and P2X7 KO respectively, ns). (h) P2X7 KO nerves expresses lower levels of CASP3 (0.624 ± 0.074) compared to WT (1.050 ± 0.155), although this was not statistically significant. CASP3 was significantly upregulated in both groups at T72 (3.123 ± 0.165 and 3.458 ± 0.191 for WT and P2X7 KO, respectively, $^{****}p < 0.0001$)

($^{***}p < 0.001$ for WT, and $^{****}p < 0.0001$ for P2X7 KO respectively Figure 4b). At T0, P2X7 KO nerves expressed significantly higher levels of PMP22 compared to WT controls ($^{***}p < 0.001$, Figure 4c); at T72, PMP22 gene expression levels were significantly decreased ($^{****}p < 0.0001$, Figure 4c). P0 expression levels were marginally higher at T0 in P2X7 KO compared to WT (ns, Figure 4d), and at T72 there was a significant decrease of expression levels in both WT ($^{**}p < 0.01$) and KO ($^{****}p < 0.0001$) nerves (Figure 4d).

We then analysed expression levels of neurotrophic factors involved in WD such as nerve growth factor (NGF) and brain derived neurotrophic factor (BDNF). BDNF expression levels were marginally higher in P2X7 KO compare to WT, although this was not statistically significant (ns, Figure 4e). In both experimental groups, BDNF levels were greatly upregulated after ex vivo degeneration ($^{****}p < 0.0001$, Figure 4e). No significant differences were observed in BDNF expression between P2X7R KO and WT at T72. Similarly, NGF levels were higher in P2X7 KO nerves compare to WT (ns, Figure 4f), and the expression of NGF was significantly increased in both groups after WD ($^{****}p < 0.0001$), with no significant differences between the two (ns, Figure 4f).

Finally, we analysed gene expression changes of apoptotic genes such as Caspase-2 (CASP2) and Capsase-3 (CASP3). CASP2 levels were similar in P2X7 KO nerves compared to WT at both T0 and T72 (ns), with only a marginal but not significant increase between the two time points within each group (ns, Figure 4g). CASP3 expression was marginally lower in P2X7 KO compared to WT nerves at T0 (ns), and significantly increased in both groups ($^{****}p < 0.0001$), without significant differences between WT and KO (Figure 4h).

### 3.4 | Re-myelination following nerve regeneration is delayed in P2X7 KO mice

To assess if the absence of P2X7R affects the capability of Schwann cells to remyelinate regenerating axons, we performed morphometric analyses of the distal stumps of regenerated nerves from WT and KO 4 and 8 weeks after the injury. The light and transmission electron microscopy analyses showed a different regenerating phenotype in peripheral nerves from injured P2X7R KO mice compared to control animals (WT). At 4 weeks after the injury, the P2X7R nerves had a significantly lower number of Remak bundles compared to WT ($^{***}p < 0.001$, Figure 5a). By week 8, the number of Remak bundles in the P2X7 KO nerves had increased significantly ($^{***}p < 0.001$) compared to 4 weeks P2X7R nerves, and was similar to WT nerves (ns). At 4 weeks, the Remak bundles in the injured KO nerves contained a significantly lower number of unmyelinated axons compared to WT ($^{***}p < 0.001$, Figure 5b), and this did not change at the 8 weeks time point (ns), where the unmyelinated axons within the KO Remak were still lower compared to 8 weeks WT controls ($^{***}p < 0.001$, Figure 5b). The effect at 4 weeks was also confirmed in transmission electron microscopy images (Figure 6a), in which the unmyelinated axons appeared lower in KO nerves compared to WT. At 4 weeks after injury we also found a higher number of single unmyelinated axons (not contained within a Remak bundle) in P2X7 KO nerves compared to WT ($^{***}p < 0.001$, Figure 5c). The number of single unmyelinated axons significantly increased in P2X7 KO nerves after further 4 weeks ($^{***}p < 0.001$), although at 8 weeks the number of single unmyelinated axons was significantly higher in WT nerves compared to P2X7 KO ($^{*}p < 0.05$, Figure 5c). This was further shown in transmission electron microscopy images (Figure 6b) still confirming a decrease in

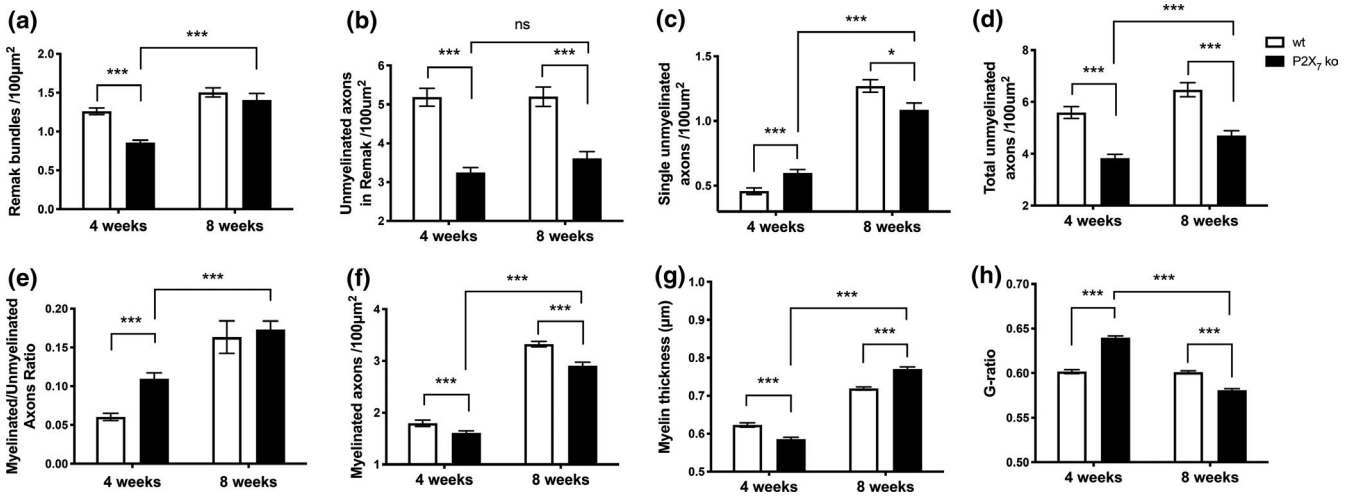


**FIGURE 5** Remyelination following injury is affected by the absence of P2X7 receptors. (a) The number of Remak bundles was lower in the distal stump of regenerating P2X7 KO nerves 4 weeks after the injury, when compared to WT (0.8595 ± 0.030 versus 1.261 ± 0.044 Rb per 100 μm$^2$, ***$p < 0.001$). After 8 weeks, the Remak bundles in P2X7 KO nerves were increased when compared to 4 weeks (***$p < 0.001$), however there was no significant difference between KO and WT nerves (1.404 ± 0.087 and 1.504 ± 0.060 Rb per 100 μm$^2$, respectively). (b) The number of unmyelinated axons contained within the Remak bundles was lower in P2X7 KO compared to WT, respectively at 4 weeks (3.246 ± 0.13 versus 5.189 ± 0.23 axons per 100 μm$^2$, ***$p < 0.001$) and 8 weeks (3.614 ± 0.17 versus 5.202 ± 0.25 axons per 100 μm$^2$, ***$p < 0.001$) after the injury. (c) Single unmyelinated axons, not contained in Remak bundles were found in higher numbers in P2X7 KO nerves at 4 weeks after the injury, when compared to WT (0.5976 ± 0.027 versus 0.4058 ± 0.025 axons per 100 μm$^2$, ***$p < 0.001$). At 8 weeks the number of single unmyelinated axons was significantly higher (*$p < 0.05$) in WT nerves compared to P2X7 KO (1.271 ± 0.048 and 1.087 ± 0.052 for WT and P2X7 KO respectively). (d) The overall number of unmyelinated axons (in Remak bundles plus single axons) was lower in P2X7 KO nerves compared to WT, respectively at 4 weeks (3.246 ± 0.13 versus 5.189 ± 0.23, ***$p < 0.001$), and 8 weeks (3.614 ± 0.17 versus 5.202 ± 0.25, ***$p < 0.001$) after injury. However, in P2X7 KO was found a weak but significant increase between 4 and 8 weeks after injury (***$p < 0.001$). (e) At 4 weeks after regeneration, the ratio between myelinated and unmyelinated fibres was higher in P2X7 KO mice versus WT (0.1098 ± 0.0073 versus 0.06049 ± 0.0047, ***$p < 0.001$). This ratio significantly increased (***$p < 0.001$) in P2X7 at the 8 week time point when compared at 4 weeks, whereas at 8 weeks here was no difference between WT and KO (0.1633 ± 0.021 and 0.1731 ± 0.011, respectively, ***$p < 0.001$). (f) The number of myelinated axons was lower in P2X7 KO compared to WT at 4 weeks (1.611 ± 0.040 versus 1.793 ± 0.062, ***$p < 0.001$) and 8 weeks (2.906 ± 0.071 versus 3.324 ± 0.054, ***$p < 0.001$), albeit the number of myelinated axons significantly increased (***$p < 0.001$) in KO nerves at 8 weeks when compared to 4 weeks post injury. (g) Myelin thickness was lower in P2X7 KO nerves compared to WT at 4 weeks after injury (0.5856 ± 0.0051 versus 0.6227 ± 0.0059, ***$p < 0.001$), however after further 4 weeks P2X7 KO nerves showed thicker myelin versus WT (0.7700 ± 0.0059 versus 0.7188 ± 0.0044, ***$p < 0.001$). In P2X7 KO, the myelin thickness augmented significantly (***$p < 0.001$), comparing the 4 to the 8 week time point. (h) The G-ratio was higher in P2X7 KO nerves compared to WT at 4 weeks (0.6396 ± 0.0020 versus 0.6016 ± 0.0022, ***$p < 0.001$), whereas it was lower in KO compared to WT at 8 weeks (0.5807 ± 0.0018 versus 0.6010 ± 0.0015, ***$p < 0.001$). Moreover, the G-ratio in P2X7 KO nerves significantly decreased between the 2 time points considered (***$p < 0.001$)

single unmyelinated fibres. Despite these changes, the total number of unmyelinated axons (both in Remaks and singles) was lower in P2X7 KO nerves compared to WT at both time points (***$p < 0.001$), while a weak but significant increase was observed in P2X7 KO between 4 and 8 weeks after injury (***$p < 0.001$, Figure 5d). Interestingly, transmission electron microscopy images showed a particular structure formed by a Schwann cell, enveloping some unmyelinated axons, and surrounding a myelinated fibre (Figure 6c). At 4 weeks after the injury the ratio between myelinated and unmyelinated axons was significantly higher in P2X7 KO mice compared to WT, (***$p < 0.001$, Figure 5e); this ratio significantly increased (***$p < 0.001$) at the 8 weeks time point (Figure 5e). The overall number of myelinated axons was significantly lower in P2X7 KO nerves compared to WT, at both time points considered (***$p < 0.001$, Figure 5f), although it significantly increased in P2X7 KO between 4 and 8 weeks after the injury (***$p < 0.001$, Figure 5f). Myelin thickness was significantly lower in P2X7 KO nerves compared to WT at 4 weeks (***$p < 0.001$, Figure 5g), and rose significantly in P2X7 KO at 8 weeks, when compared to WT (***$p < 0.001$, Figure 5g). Interestingly, myelin thickness augmented significantly in P2X7 KO nerves comparing the 4 to the 8 weeks time point (***$p < 0.001$, Figure 5g; see also Figure 6a,b). Conversely, in P2X7 KO nerves the G-ratio was higher than WT at 4 weeks after injury and lower than WT after 8 weeks, with a significant decrease between the 2 time points (***$p < 0.001$, Figure 5h). Finally, an increase in the percentage of irregular fibres (IC lower than 0.75) was found in P2X7 KO nerves at 4 weeks (65% in KO versus 47% in

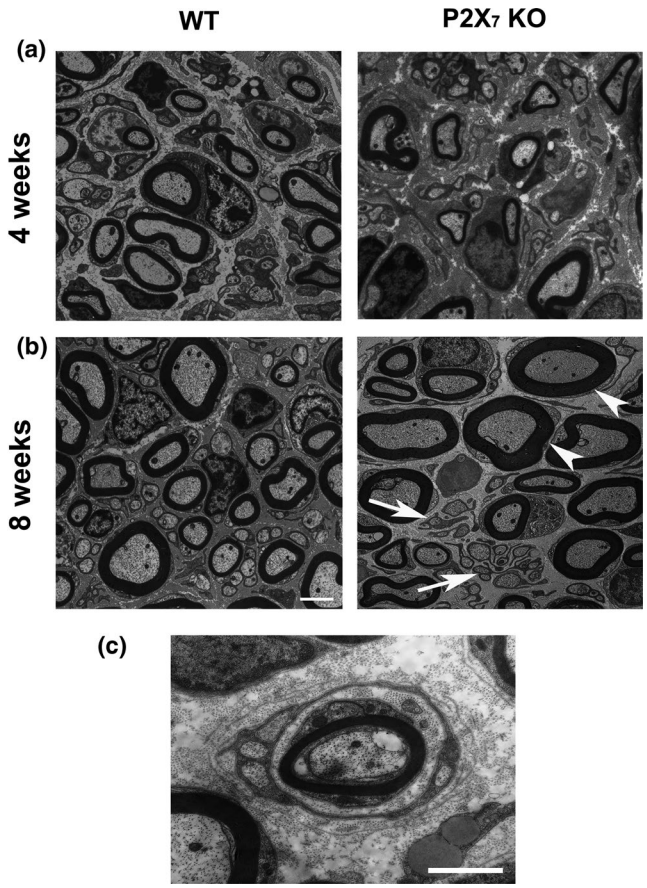


**FIGURE 6** Electron microscopy images from WT and P2X7 KO cross-sectioned nerves following injury and repair. Comparison between nerve cross-sections of WT and P2X7 KO mice at 4 (a) and 8 (b) weeks post injury showing thicker myelinated fibers in P2X7 KO mice at 8 weeks (white arrowheads), and a lower number of single unmyelinated axons (white arrows) compared to WT. (c) Electron micrograph from a cross-section of P2X7 sciatic nerve 4 weeks post injury, showing a Schwann cell enveloping some unmyelinated axons that surrounds a myelinated fiber. Scale bars 5μm

WT), although this difference flattened at 8 weeks (P2X7 KO nerves 76% versus WT 79%).

## 4 | DISCUSSION

Pharmaceutical therapies for peripheral nerve injury are currently unavailable. A large number of pharmaceutical targets have been proposed as promising candidates for the development of novel therapies for peripheral nerve regeneration. In particular, extensive research has been focusing on neurotransmitters such as GABA, ATP and Ach, and their receptors, as systems to be targeted. In previous work, we have shown how GABA receptors play important roles in determining the fate of Schwann cells during development (Faroni & Magnaghi, 2011; Magnaghi et al., 2009). Indeed, mice lacking GABA-B1 receptors in the whole organism (Magnaghi et al., 2008), or selectively in Schwann cells (Faroni, Castelnovo, et al., 2014), showed an altered phenotype of peripheral nerve morphology and phenotype, highlighting the importance of GABA-B1 receptors for the SC commitment to a non-myelinating phenotype. This was also confirmed with in vitro cultures of SC and DRG neurons from GABA-B1 knockout animals (Faroni et al., 2019). Treatment with GABA ligands modulates the production and release of neurotrophins in SC in vitro (Faroni, Calabrese, et al., 2013), and promotes nerve regeneration in a sciatic nerve lesion model in vivo (Magnaghi et al., 2014). Ach signaling has also been extensively associated with the regulation of myelination, and particularly more recently with the regulation of Schwann cell physiology during development and remyelination following injury (Fields et al., 2017). Indeed, Schwann cells express several muscarinic receptors, with M2 being specifically important for Schwann cell proliferation and myelin formation (Loreti et al., 2006, 2007; Uggenti et al., 2014). Similarly, purinergic receptors for ATP have been identified in several glial cells, including Schwann cells, where they take part in several neuron-glia interactions that are fundamental for glial cell pathophysiology (Fields & Burnstock, 2006; Fields & Stevens, 2000; Lecca et al., 2012; Verkhratsky et al., 2009). Indeed, Schwann cells located along axon segments respond to ATP and other neurotransmitters released by axons during electrical stimulation, which in turn may affect Schwann cell proliferation, differentiation, and myelination (Fields & Burnstock, 2006; Fields et al., 2017; Fields & Stevens, 2000; Fields & Stevens-Graham, 2002; Stevens & Fields, 2000; Stevens et al., 1998, 2002). Furthermore, several cellular mechanisms for ATP release, including P2X7R, have been identified in non-neuronal cells (Fields, 2011).

In a previous study, we demonstrated that P2X7 receptors localise mainly in myelinating Schwann cells in the PNS. Moreover we showed that peripheral nerves from P2X7 KO mice possess an altered molecular and morphological phenotype, suggesting a key role for P2X7R to determine Schwann cell fate during development (Faroni, Smith, et al., 2014). This peculiar phenotype results was described in the P2X7 KO mice developed by GSK, (Chessell et al., 2005); however, Pfizer developed a similar knockout model (Solle et al., 2001), which showed similar but not identical characteristics (Sim et al., 2004). For this reason, in the current work we repeated some of the initial characterisation of the peripheral nerves phenotype studied in GSK P2X7 KO (Faroni, Smith, et al., 2014), also in the Pfizer mice developed by Solle et al. (Solle et al., 2001). As in the GSK P2X7 KO model (Faroni, Smith, et al., 2014), Pfizer P2X7 KO mice also showed reduced expression of myelin proteins P0, MBP and MAG, as well as featuring the main morphometric properties of the GSK model (increased number of Remak and unmyelinated axons, as well as irregular fibres).

Furthermore, in this study, we focused on the role or P2X7 receptor during injury and repair. Using ex vivo and in vivo models of nerve regeneration, we found that the absence of P2X7R does not affect the degenerative phase (Wallerian degeneration) that follows nerve injury and does not influence the speed of axonal regeneration. Nevertheless, EM studies showed that re-myelination is delayed in P2X7 KO mice, suggesting a role for P2X7R in the determination of the myelinating phenotype in injury and repair, in the same way it does during development. Indeed, KO mice showed a lower number of myelinated axons compared to WT at both 4 weeks and 8 weeks after the injury and repair. The number of Remak bundles was also lower in KO nerves 4 weeks after injury, although there was no difference in number of Remak after 8 weeks between WT and P2X7 KO. Additionally, the Remak bundles in regenerating KO nerves contained a lower number of unmyelinated axons at both 4 and 8 weeks after injury. Interestingly, at 4 weeks during regeneration we found an increased number of single unmyelinated axons (not belonging to Remak) in KO nerves compared to WT, with an inverted trend at 8 weeks. We believe that the increased number of single unmyelinated axons at 4 weeks is a feature of delayed re-myelination. Indeed, these axons could have been sorted for myelination, but yet to be myelinated. At 8 weeks following the repair the situation is inverted with a higher number of single unmyelinated axons in the WT compared to the controls. We can speculate that beside being delayed, myelination is also generally hindered in the absence of P2X7R. Indeed, this would explain the higher number of unmyelinated single axons in WT at 8 weeks, with a re-myelination program that is still active in WT mice, but delayed in P2X7 KO. The slower re-myelination profile in the KO mice is also further confirmed by the reduced number of myelinated axons at both 4 and 8 weeks, compared to WT. Overall, the radial sorting is a developmental physiologic process in which the Schwann cells choose mostly larger axons to myelinate. Radial sorting defects may occur in neuropathologic complications of the PNS. Interestingly, our observations corroborate the evidence that P2X7R might have a role in regulating the radial sorting process (Feltri et al., 2016), as shown by the presence of structures composed of unmyelinated axons surrounding a myelinated fibre (electron micrographs), typical sign of morphological defects in radial sorting (Feltri et al., 2016).

Furthermore, myelin thickness is lower in KO at 4 weeks; this is because the higher number of single unmyelinated (or lightly myelinated) axons causes the overall thinning of myelin thickness. This is further confirmation that myelination is delayed, together with the lower number of myelinated axons at both time points. Myelin thickness is higher in P2X7 KO nerves at 8 weeks. Similarly to what stated before, myelination is not only delayed in KO, but might also last less in general. Indeed, if this was the case the more active myelination program in WT would cause the overall myelin thickness to be lower at 8 weeks (due to an increased number of single unmyelinated/lightly myelinated axons still actively myelinating). Altogether, these complicated findings point towards the conclusion that re-myelination is delayed and globally hindered in the absence of P2X7 receptors.

In the acute phase following peripheral nerve injury, expression of P2X7R is upregulated in Schwann cells, which is associated with Schwann cell proliferation mediated by ATP (Song et al., 2015). With respect to demyelinating neuropathies, Schwann cells taken from a rat model of Charcot-Marie-Tooth 1A show abnormally high intracellular $Ca^{2+}$ concentration due to overexpression of P2X7R mediated by peripheral myelin protein 22 (PMP22). In this animal model, the P2X7R reversible antagonist A438079 improved myelination in both in vitro organic DRG cultures, and in vivo histologic analysis. Consequentially these animals showed significant improvements in muscle strength and distal motor latencies compared to placebo controls, however, compound muscle action potentials remained unaltered (Sociali et al., 2016). Studies in rat Schwann cells have shown that exposure to high concentrations of ATP or P2X7R agonists (BzATP) induce significant rapid cell death, increasing membrane permeability to large molecules including ethidium. Furthermore, these responses were not seen with irreversible (oxaTP) or reversible (A438079) antagonists, or in P2X7R KO mice, therefore suggesting that P2X7R is responsible for ATP-induced Schwann cell death in vitro (Faroni, Rothwell, et al., 2013; Luo et al., 2013). Considering that ATP is present in high concentrations at the injury site, P2X7R is likely to be a mediator of Schwann cell death following injury.

Following nerve transection, structural proteins such as P0, PMP22, MAG and MBP are all rapidly downregulated (Mirsky & Jessen, 1999). On the contrary, neurotrophic factors such as NGF and BDNF are all upregulated, enabling axonal elongation and neuronal survival (Chen et al., 2007). Neurotrophins, such as NGF and BDNF, are fundamental in the guidance of axonal elongation following peripheral nerve injury (Jessen & Mirsky, 2016). Interestingly, at T0 the P2X7 KO had a higher expression of all myelin proteins (i.e. P0, PMP22, MBP, MAG) compared to WT, corroborating the hypothesis of a strong correlation between the P2X7R and myelin proteins, and its involvement in nerve myelination (Faroni, Smith, et al., 2014; Nobbio et al., 2009). In this study, following 72 hr of in vitro degeneration, we successfully recapitulated several aspects of in vivo WD, including the downregulation of myelin proteins and the upregulation of neurotrophic growth factors (Faroni et al., 2015). Moreover 72 hr of in vitro WD also increased cell death, according to in vivo (Faroni et al., 2015). Indeed, expression of both caspase 2 and caspase 3, which function as central regulators of cell death (D'Amelio et al., 2010), increased after injury and ex vivo degeneration, suggesting that cell death is occurring.

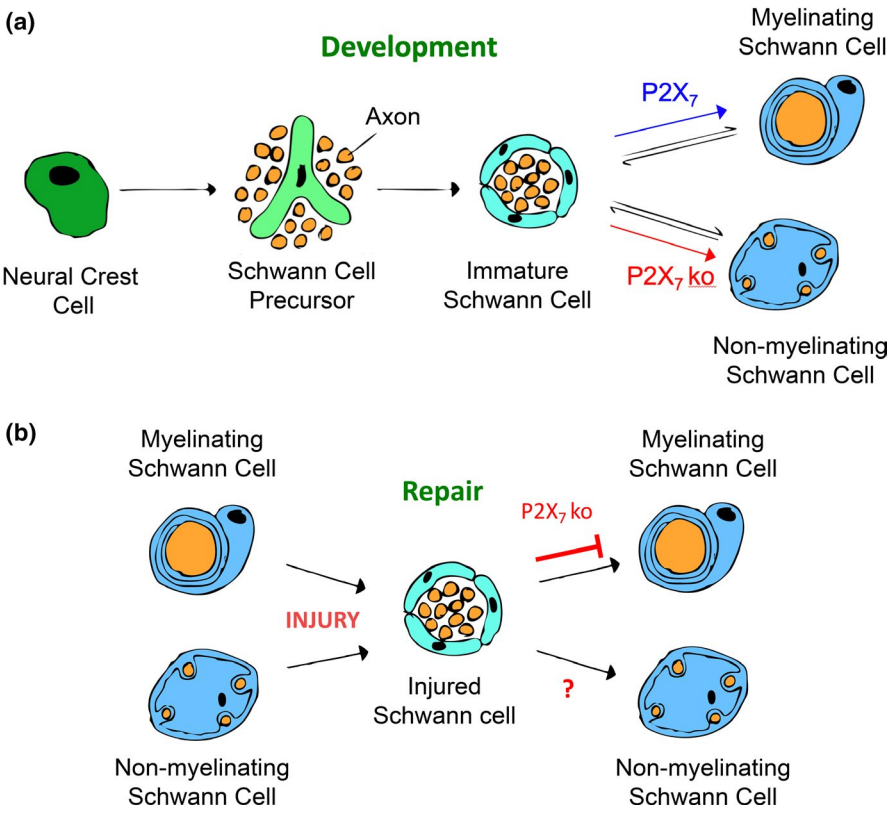


**FIGURE 7** The role of P2X7 receptor on peripheral nerve development and regeneration (a) During development, Schwan cells, deriving from the neural crest, can differentiate towards a myelinating or non-myelinating phenotype. P2X7 receptors play a role in the determination of SC fate; indeed, mice lacking P2X7R possess higher number of unmyelinated fibres in the peripheral nerves, with a lower number of myelinated axons, suggesting that P2X7 receptors are essential for the transition of Schwann cells from immature to a myelinating phenotype (Faroni, Smith, et al., 2014). (b) Following injury and during Wallerian degeneration, both myelinating and non-myelinating Schwann cells loose contact with the axons and de-differentiate into a "repair" phenotype which drives nerve regeneration (Jessen & Mirsky, 2016). After the nerve is regenerated the repair Schwann cells re-differentiate into myelinating or non-myelinating Schwann. Herein, we showed that the absence of P2X7R does not affect the Wallerian degeneration phase following nerve injury. Furthermore, speed of nerve regrowth is unaltered in P2X7 KO mice, compared to controls. Nevertheless, lack of P2X7 receptors hinders the re-myelinating potential of repair Schwann cells resulting in delayed and less effective remyelination

Caspase 3 showed a higher degree of upregulation in gene expression levels compared to caspase 2 in both WT and P2X7 KO nerves. Hanley et al. suggested that caspase 3 activation is ATP-concentration dependent and thus may be downstream of the P2X7R (Hanley et al., 2012). Nevertheless, caspase 3 mediated cell death is independent of other apoptosis pathways, such as caspase-1 (Hanley et al., 2012), and therefore other cell death mechanisms might be occurring. The activation of both caspase-3 and P2X7R is known to lead to membrane blebbing and subsequent cell death, via the degradation of cytoskeleton proteins (Janicke et al., 1998). Importantly, some of these changes also reflected on the DRGs, in which inflammatory mediators (e.g. NFkB, TNFα, etc.) increased following nerve transection, both in WT and P2X7 KO. Gene expression changes in DRGs following peripheral nerve transection are part of the pathophysiological response of the PNS to nerve injury (Martin et al., 2019). As NFκB is ubiquitously expressed, the increase observed in the P2X7 KO may highlight an increased recruitment of inflammatory cells to the DRG, compared to the WT. Inflammation is required to clear the cellular debris and improve the environment for regeneration, however, it also increases cellular death and can counterbalance the recovery (Rock, 2009). Indeed, TNF is an apoptotic mediator, associated with a variety of other roles, including necrosis (Bradley, 2008), and DRG excitability determining neuropathic pain (Zhang et al., 2007). The TNFα pro-apoptotic effect was also associated to upregulation of caspase-2 and caspase-3, implying that an increase in cell death also occurred.

Nevertheless, in the DRGs we also found upregulation of factors that oppose the increase of cell death mediators, such as the transcription factor ATF3 or the neuropeptide galanin which are reported to improve neuronal survival after injury (Hobson et al., 2008; Holmberg et al., 2005). ATF3 is generally considered a marker of nerve injury, indeed naïve animals have a very low expression of ATF3 in the DRG neurons, while an injury induces its high upregulation (Tsujino et al., 2000). Given that ATF3 has a role in controlling the

expression of other genes that are important for recovery, it is one of the earliest genes to be upregulated following an injury (Hyatt Sachs et al., 2007). Moreover, galanin upregulation after injury is also in accordance to data on injured superior cervical ganglia (Schreiber et al., 1994). It is known that galanin is predominantly located in the small/medium neurons within the DRG, whereas P2X7R is mainly found in the surrounding glial cells, which suggests important functions for neuron-glia communication (Zhang et al., 2007). Hence, in order to unveil the signalling cascade triggering the galanin gene expression increase, we hypothesised that the altered gene expression of galanin may be a result of the loss of this communication mechanism. Finally, we found that growth factors were upregulated in DRGs after injury, likely in order to promote axonal elongation. Indeed, it is well established that NGF is upregulated after injury in DRG (Lindsay, 1988; McMahon, 1996; Woolf & Costigan, 1999), and is vital for recovery of the DRG neurons (Lindsay, 1988). However, NGF exerts important roles in the neuroregenerative process as well as in the neuroinflammatory response within the adult DRG sensory neurons (McMahon, 1996; Woolf & Costigan, 1999). The drop in NGF expression has also been correlated with the increase in galanin (Rao et al., 1993; Shadiack et al., 1998).

Collectively, our findings point to the role of P2X7R in the determination of Schwann cell fate, facilitating the transition of Schwann cells from immature to a myelinating phenotype (Figure 7; Lindsay, 1988; McMahon, 1996; Woolf & Costigan, 1999). Namely, these receptors support the regeneration and re-myelination following peripheral nerve injury and in demyelinating neuropathies. More work needs to be done to understand the the role of P2X7R in non-myelinating Schwann cells, and to exploit P2X7 receptors as potential pharmacological targets for novel nerve repair strategies.

## ACKNOWLEDGEMENTS

AF and AJR are supported by the Hargreaves and Ball Trust, the Academy of Medical Sciences (AMS-SGCL7), and by Seed Corn Funding from the Rosetrees Trust and the Stoneygate Trust (M746). The authors thank Prof. Patriza Procacci for the precious help in setting up the morphometric analysis and to Emily May Fisher for the analyses of the *ex vivo* model.

## CONFLICTS OF INTEREST

The authors declare no competing financial or commercial interest.

## AUTHORS CONTRIBUTION

V.M., A.F., S.M, P.S., and L.A. performed in vivo experiments, immunofluorescence, and gene expression studies. V.C. and P.S. performed electron microscopy and image analysis. A.F. and A.J.R. did statistic. Study was designed by A.F., with assistance of V.M. and A.J.R. The manuscript written by V.M and A.F. with assistance of A.J.R.

## DATA AVAILABILITY STATEMENT

The datasets generated during and/or analysed during the current study are available from the corresponding author on reasonable request.

## PEER REVIEW

The peer review history for this article is available at https://publons.com/publon/10.1111/ejn.14995.

## ORCID

*Valerio Magnaghi* https://orcid.org/0000-0002-6903-7042
*Adam J. Reid* https://orcid.org/0000-0003-1752-3302
*Alessandro Faroni* https://orcid.org/0000-0003-4435-6423

## REFERENCES

Allen-Jennings, A. E., Hartman, M. G., Kociba, G. J., & Hai, T. (2001). The roles of ATF3 in glucose homeostasis. A transgenic mouse model with liver dysfunction and defects in endocrine pancreas. *Journal of Biological Chemistry*, *276*, 29507–29514. https://doi.org/10.1074/jbc.M100986200

Bradley, J. R. (2008). TNF-mediated inflammatory disease. *The Journal of Pathology*, *214*, 149–160.

Chen, Z. L., Yu, W. M., & Strickland, S. (2007). Peripheral regeneration. *Annual Review of Neuroscience*, *30*, 209–233. https://doi.org/10.1146/annurev.neuro.30.051606.094337

Chessell, I. P., Hatcher, J. P., Bountra, C., Michel, A. D., Hughes, J. P., Green, P., Egerton, J., Murfin, M., Richardson, J., Peck, W. L., Grahames, C. B., Casula, M. A., Yiangou, Y., Birch, R., Anand, P., & Buell, G. N. (2005). Disruption of the P2X7 purinoceptor gene abolishes chronic inflammatory and neuropathic pain. *Pain*, *114*, 386–396. https://doi.org/10.1016/j.pain.2005.01.002

Cunningham, P. N., Dyanov, H. M., Park, P., Wang, J., Newell, K. A., & Quigg, R. J. (2002). Acute renal failure in endotoxemia is caused by TNF acting directly on TNF receptor-1 in kidney. *Journal of Immunology*, *168*, 5817–5823. https://doi.org/10.4049/jimmunol.168.11.5817

D'Amelio, M., Cavallucci, V., & Cecconi, F. (2010). Neuronal caspase-3 signaling: Not only cell death. *Cell Death and Differentiation*, *17*, 1104–1114. https://doi.org/10.1038/cdd.2009.180

Faroni, A., Calabrese, F., Riva, M. A., Terenghi, G., & Magnaghi, V. (2013). Baclofen modulates the expression and release of neurotrophins in Schwann-like adipose stem cells. *Journal of Molecular Neuroscience*, *49*, 233–243. https://doi.org/10.1007/s12031-012-9813-6

Faroni, A., Castelnovo, L. F., Procacci, P., Caffino, L., Fumagalli, F., Melfi, S., Gambarotta, G., Bettler, B., Wrabetz, L., & Magnaghi, V. (2014). Deletion of GABA-B receptor in Schwann cells regulates remak bundles and small nociceptive C-fibers. *Glia*, *62*, 548–565. https://doi.org/10.1002/glia.22625

Faroni, A., & Magnaghi, V. (2011). The neurosteroid allopregnanolone modulates specific functions in central and peripheral glial cells. *Frontiers in Endocrinology*, *2*, 103. https://doi.org/10.3389/fendo.2011.00103

Faroni, A., Melfi, S., Castelnovo, L. F., Bonalume, V., Colleoni, D., Magni, P., Arauzo-Bravo, M. J., Reinbold, R., & Magnaghi, V. (2019). GABA-B1 receptor-null Schwann cells exhibit compromised in vitro myelination. *Molecular Neurobiology*, *56*, 1461–1474. https://doi.org/10.1007/s12035-018-1158-x

Faroni, A., Mobasseri, S. A., Kingham, P. J., & Reid, A. J. (2015). Peripheral nerve regeneration: Experimental strategies and future perspectives. *Advanced Drug Delivery Reviews*, *82–83*, 160–167. https://doi.org/10.1016/j.addr.2014.11.010

Faroni, A., Rothwell, S. W., Grolla, A. A., Terenghi, G., Magnaghi, V., & Verkhratsky, A. (2013). Differentiation of adipose-derived stem cells into Schwann cell phenotype induces expression of P2X receptors that control cell death. *Cell Death & Disease*, *4*, e743. https://doi.org/10.1038/cddis.2013.268

Faroni, A., Smith, R. J., Procacci, P., Castelnovo, L. F., Puccianti, E., Reid, A. J., Magnaghi, V., & Verkhratsky, A. (2014). Purinergic signaling mediated by P2X7 receptors controls myelination in sciatic nerves. *Journal of Neuroscience Research*, *92*, 1259–1269.

Feltri, M. L., Poitelon, Y., & Previtali, S. C. (2016). How Schwann cells sort axons: New concepts. *Neuroscientist*, *22*, 252–265. https://doi.org/10.1177/1073858415572361

Fields, R. D. (2011). Nonsynaptic and nonvesicular ATP release from neurons and relevance to neuron-glia signaling. *Seminars in Cell & Developmental Biology*, *22*, 214–219. https://doi.org/10.1016/j.semcdb.2011.02.009

Fields, R. D., & Burnstock, G. (2006). Purinergic signalling in neuron-glia interactions. *Nature Reviews Neuroscience*, *7*, 423–436. https://doi.org/10.1038/nrn1928

Fields, R. D., Dutta, D. J., Belgrad, J., & Robnett, M. (2017). Cholinergic signaling in myelination. *Glia*, *65*, 687–698. https://doi.org/10.1002/glia.23101

Fields, R. D., & Stevens, B. (2000). ATP: An extracellular signaling molecule between neurons and glia. *Trends in Neurosciences*, *23*, 625–633. https://doi.org/10.1016/S0166-2236(00)01674-X

Fields, R. D., & Stevens-Graham, B. (2002). New insights into neuron-glia communication. *Science*, *298*, 556–562. https://doi.org/10.1126/science.298.5593.556

Gesing, A., Wang, F., List, E. O., Berryman, D. E., Masternak, M. M., Lewinski, A., Karbownik-Lewinska, M., Kopchick, J. J., & Bartke, A. (2015). Expression of apoptosis-related genes in liver-specific growth hormone receptor gene-disrupted mice is sex dependent. *Journals of Gerontology. Series A, Biological Sciences and Medical Sciences*, *70*, 44–52. https://doi.org/10.1093/gerona/glu008

Hanley, P. J., Kronlage, M., Kirschning, C., del Rey, A., Di Virgilio, F., Leipziger, J., Chessell, I. P., Sargin, S., Filippov, M. A., Lindemann, O., Mohr, S., Konigs, V., Schillers, H., Bahler, M., & Schwab, A. (2012). Transient P2X7 receptor activation triggers macrophage death independent of Toll-like receptors 2 and 4, caspase-1, and pannexin-1 proteins. *Journal of Biological Chemistry*, *287*, 10650–10663.

Hanoux, V., Pairault, C., Bakalska, M., Habert, R., & Livera, G. (2007). Caspase-2 involvement during ionizing radiation-induced oocyte death in the mouse ovary. *Cell Death and Differentiation*, *14*, 671–681. https://doi.org/10.1038/sj.cdd.4402052

He, B., Counts, S. E., Perez, S. E., Hohmann, J. G., Koprich, J. B., Lipton, J. W., Steiner, R. A., Crawley, J. N., & Mufson, E. J. (2005). Ectopic galanin expression and normal galanin receptor 2 and galanin receptor 3 mRNA levels in the forebrain of galanin transgenic mice. *Neuroscience*, *133*, 371–380. https://doi.org/10.1016/j.neuroscience.2005.01.068

Hobson, S. A., Bacon, A., Elliot-Hunt, C. R., Holmes, F. E., Kerr, N. C., Pope, R., Vanderplank, P., & Wynick, D. (2008). Galanin acts as a trophic factor to the central and peripheral nervous systems. *Cellular and Molecular Life Sciences*, *65*, 1806–1812.

Holmberg, K., Kuteeva, E., Brumovsky, P., Kahl, U., Karlstrom, H., Lucas, G. A., Rodriguez, J., Westerblad, H., Hilke, S., Theodorsson, E., Berge, O. G., Lendahl, U., Bartfai, T., & Hokfelt, T. (2005). Generation and phenotypic characterization of a galanin overexpressing mouse. *Neuroscience*, *133*, 59–77. https://doi.org/10.1016/j.neuroscience.2005.01.062

Hyatt Sachs, H., Schreiber, R. C., Shoemaker, S. E., Sabe, A., Reed, E., & Zigmond, R. E. (2007). Activating transcription factor 3 induction in sympathetic neurons after axotomy: Response to decreased neurotrophin availability. *Neuroscience*, *150*, 887–897. https://doi.org/10.1016/j.neuroscience.2007.10.008

Janicke, R. U., Sprengart, M. L., Wati, M. R., & Porter, A. G. (1998). Caspase-3 is required for DNA fragmentation and morphological changes associated with apoptosis. *Journal of Biological Chemistry*, *273*, 9357–9360. https://doi.org/10.1074/jbc.273.16.9357

Jessen, K. R., & Mirsky, R. (2016). The repair Schwann cell and its function in regenerating nerves. *Journal of Physiology*, *594*, 3521–3531. https://doi.org/10.1113/JP270874

Lecca, D., Ceruti, S., Fumagalli, M., & Abbracchio, M. P. (2012). Purinergic trophic signalling in glial cells: Functional effects and modulation of cell proliferation, differentiation, and death. *Purinergic Signalling*, *8*, 539–557. https://doi.org/10.1007/s11302-012-9310-y

Lindsay, R. M. (1988). Nerve growth factors (NGF, BDNF) enhance axonal regeneration but are not required for survival of adult sensory neurons. *Journal of Neuroscience*, *8*, 2394–2405. https://doi.org/10.1523/JNEUROSCI.08-07-02394.1988

Loreti, S., Ricordy, R., De Stefano, M. E., Augusti-Tocco, G., & Tata, A. M. (2007). Acetylcholine inhibits cell cycle progression in rat Schwann cells by activation of the M2 receptor subtype. *Neuron Glia Biology*, *3*, 269–279. https://doi.org/10.1017/S1740925X08000045

Loreti, S., Vilaro, M. T., Visentin, S., Rees, H., Levey, A. I., & Tata, A. M. (2006). Rat Schwann cells express M1–M4 muscarinic receptor subtypes. *Journal of Neuroscience Research*, *84*, 97–105. https://doi.org/10.1002/jnr.20874

Luo, J., Lee, S., Wu, D., Yeh, J., Ellamushi, H., Wheeler, A. P., Warnes, G., Zhang, Y., & Bo, X. (2013). P2X7 purinoceptors contribute to the death of Schwann cells transplanted into the spinal cord. *Cell Death & Disease*, *4*, e829. https://doi.org/10.1038/cddis.2013.343

Magnaghi, V., Ballabio, M., Camozzi, F., Colleoni, M., Consoli, A., Gassmann, M., Lauria, G., Motta, M., Procacci, P., Trovato, A. E., & Bettler, B. (2008). Altered peripheral myelination in mice lacking GABAB receptors. *Molecular and Cellular Neurosciences*, *37*, 599–609. https://doi.org/10.1016/j.mcn.2007.12.009

Magnaghi, V., Castelnovo, L. F., Faroni, A., Cavalli, E., Caffino, L., Colciago, A., Procacci, P., & Pajardi, G. (2014). Nerve regenerative effects of GABA-B ligands in a model of neuropathic pain. *BioMed Research International*, *2014*, 368678. https://doi.org/10.1155/2014/368678

Magnaghi, V., Procacci, P., & Tata, A. M. (2009) Chapter 15: Novel pharmacological approaches to Schwann cells as neuroprotective agents for peripheral nerve regeneration. *International Review of Neurobiology*, *87*, 295–315.

Martin, S. L., Reid, A. J., Verkhratsky, A., Magnaghi, V., & Faroni, A. (2019). Gene expression changes in dorsal root ganglia following peripheral nerve injury: Roles in inflammation, cell death and nociception. *Neural Regeneration Research*, *14*, 939–947. https://doi.org/10.4103/1673-5374.250566

Martinez de Albornoz, P., Delgado, P. J., Forriol, F., & Maffulli, N. (2011). Non-surgical therapies for peripheral nerve injury. *British Medical Bulletin*, *100*, 73–100. https://doi.org/10.1093/bmb/ldr005

Mayhew, T. M., & Sharma, A. K. (1984). Sampling schemes for estimating nerve fibre size. I. Methods for nerve trunks of mixed fascicularity. *Journal of Anatomy*, *139*(Pt 1), 45–58.

McMahon, S. B. (1996). NGF as a mediator of inflammatory pain. *Philosophical Transactions of the Royal Society of London. Series B, Biological Sciences*, *351*, 431–440.

Mirsky, R., & Jessen, K. R. (1999). The neurobiology of Schwann cells. *Brain Pathology*, *9*, 293–311. https://doi.org/10.1111/j.1750-3639.1999.tb00228.x

Nagajyothi, F., Desruisseaux, M. S., Machado, F. S., Upadhya, R., Zhao, D., Schwartz, G. J., Teixeira, M. M., Albanese, C., Lisanti, M. P., Chua, S. C. Jr, Weiss, L. M., Scherer, P. E., & Tanowitz, H. B. (2012). Response of adipose tissue to early infection with Trypanosoma cruzi (Brazil strain). *Journal of Infectious Diseases*, *205*, 830–840. https://doi.org/10.1093/infdis/jir840

Namsolleck, P., Boato, F., Schwengel, K., Paulis, L., Matho, K. S., Geurts, N., Thone-Reineke, C., Lucht, K., Seidel, K., Hallberg, A., Dahlof, B., Unger, T., Hendrix, S., & Steckelings, U. M. (2013). AT2-receptor stimulation enhances axonal plasticity after spinal cord injury by upregulating BDNF expression. *Neurobiology of Diseases*, *51*, 177–191. https://doi.org/10.1016/j.nbd.2012.11.008

Nobbio, L., Sturla, L., Fiorese, F., Usai, C., Basile, G., Moreschi, I., Benvenuto, F., Zocchi, E., De Flora, A., Schenone, A., & Bruzzone, S. (2009). P2X7-mediated increased intracellular calcium causes functional derangement in Schwann cells from rats with CMT1A neuropathy. *Journal of Biological Chemistry*, *284*, 23146–23158. https://doi.org/10.1074/jbc.M109.027128

Rao, M. S., Sun, Y., Vaidyanathan, U., Landis, S. C., & Zigmond, R. E. (1993). Regulation of substance P is similar to that of vasoactive intestinal peptide after axotomy or explantation of the rat superior cervical ganglion. *Journal of Neurobiology*, *24*, 571–580. https://doi.org/10.1002/neu.480240504

Rock, K. L. (2009). Pathobiology of inflammation to cell death. *Biology of Blood and Marrow Transplantation*, *15*, 137–138. https://doi.org/10.1016/j.bbmt.2008.11.007

Schreiber, R. C., Hyatt-Sachs, H., Bennett, T. A., & Zigmond, R. E. (1994). Galanin expression increases in adult rat sympathetic neurons after axotomy. *Neuroscience*, *60*, 17–27. https://doi.org/10.1016/0306-4522(94)90200-3

Shadiack, A. M., Vaccariello, S. A., Sun, Y., & Zigmond, R. E. (1998). Nerve growth factor inhibits sympathetic neurons' response to an injury cytokine. *Proceedings of the National Academy of Sciences of the United States of America*, *95*, 7727–7730. https://doi.org/10.1073/pnas.95.13.7727

Sim, J. A., Young, M. T., Sung, H. Y., North, R. A., & Surprenant, A. (2004). Reanalysis of P2X7 receptor expression in rodent brain. *Journal of Neuroscience*, *24*, 6307–6314. https://doi.org/10.1523/JNEUROSCI.1469-04.2004

Sociali, G., Visigalli, D., Prukop, T., Cervellini, I., Mannino, E., Venturi, C., Bruzzone, S., Sereda, M. W., & Schenone, A. (2016). Tolerability and efficacy study of P2X7 inhibition in experimental Charcot-Marie-Tooth type 1A (CMT1A) neuropathy. *Neurobiology of Diseases*, *95*, 145–157. https://doi.org/10.1016/j.nbd.2016.07.017

Solle, M., Labasi, J., Perregaux, D. G., Stam, E., Petrushova, N., Koller, B. H., Griffiths, R. J., & Gabel, C. A. (2001). Altered cytokine production in mice lacking P2X(7) receptors. *Journal of Biological Chemistry*, *276*, 125–132.

Song, X. M., Xu, X. H., Zhu, J., Guo, Z., Li, J., He, C., Burnstock, G., Yuan, H., & Xiang, Z. (2015). Up-regulation of P2X7 receptors mediating proliferation of Schwann cells after sciatic nerve injury. *Purinergic Signalling*, *11*, 203–213. https://doi.org/10.1007/s11302-015-9445-8

Stevens, B., & Fields, R. D. (2000). Response of Schwann cells to action potentials in development. *Science*, *287*, 2267–2271. https://doi.org/10.1126/science.287.5461.2267

Stevens, B., Porta, S., Haak, L. L., Gallo, V., & Fields, R. D. (2002). Adenosine: A neuron-glial transmitter promoting myelination in the CNS in response to action potentials. *Neuron*, *36*, 855–868. https://doi.org/10.1016/S0896-6273(02)01067-X

Stevens, B., Tanner, S., & Fields, R. D. (1998). Control of myelination by specific patterns of neural impulses. *Journal of Neuroscience*, *18*, 9303–9311. https://doi.org/10.1523/JNEUROSCI.18-22-09303.1998

Tsujino, H., Kondo, E., Fukuoka, T., Dai, Y., Tokunaga, A., Miki, K., Yonenobu, K., Ochi, T., & Noguchi, K. (2000). Activating transcription factor 3 (ATF3) induction by axotomy in sensory and motoneurons: A novel neuronal marker of nerve injury. *Molecular and Cellular Neurosciences*, *15*, 170–182. https://doi.org/10.1006/mcne.1999.0814

Uggenti, C., De Stefano, M. E., Costantino, M., Loreti, S., Pisano, A., Avallone, B., Talora, C., Magnaghi, V., & Tata, A. M. (2014). M2 muscarinic receptor activation regulates Schwann cell differentiation and myelin organization. *Developmental Neurobiology*, *74*, 676–691. https://doi.org/10.1002/dneu.22161

Verkhratsky, A., Krishtal, O. A., & Burnstock, G. (2009). Purinoceptors on neuroglia. *Molecular Neurobiology*, *39*, 190–208. https://doi.org/10.1007/s12035-009-8063-2

Woolf, C. J., & Costigan, M. (1999). Transcriptional and posttranslational plasticity and the generation of inflammatory pain. *Proceedings of the National Academy of Sciences of the United States of America*, *96*, 7723–7730. https://doi.org/10.1073/pnas.96.14.7723

Zhang, X., Chen, Y., Wang, C., & Huang, L. Y. (2007). Neuronal somatic ATP release triggers neuron-satellite glial cell communication in dorsal root ganglia. *Proceedings of the National Academy of Sciences of the United States of America*, *104*, 9864–9869. https://doi.org/10.1073/pnas.0611048104

Zochodne, D. W. (2012). The challenges and beauty of peripheral nerve regrowth. *Journal of the Peripheral Nervous System*, *17*, 1–18. https://doi.org/10.1111/j.1529-8027.2012.00378.x

**How to cite this article:** Magnaghi, V., Martin, S., Smith, P., Allen, L., Conte, V., Reid, A. J., & Faroni, A. (2021). Peripheral nerve regeneration following injury is altered in mice lacking P2X7 receptor. *European Journal of Neuroscience*, *54*(5), 5798–5814. https://doi.org/10.1111/ejn.14995